ON THE ACCURACY OF THE TOMOGRAPHIC GAMMA SCANNER FOR THE ASSAY OF DRUMMED WASTE

S. Croft, R.Venkataraman, M.Villani
Canberra Industries, Inc.
800 Research Parkway, Meriden, Connecticut, 06450, USA.

R. J. Estep
Advanced Nuclear Technology Group (NIS-6), Los Alamos National Laboratory
Los Alamos, New Mexico 87545, USA.

ABSTRACT

The Tomographic Gamma Scanner (TGS) [1] combines high-resolution gamma spectrometry with low-resolution 3-dimensional reconstructive transmission and emission imagery for the Non Destructive Assay (NDA) of gamma emitting items. In the chronology of NDA instrumentation the TGS is a relative new comer and only a small number such systems have been deployed for the routine processing of drummed radioactive waste. Consequently little information is available in the literature regarding the accuracy of the method - be it state of the art or state of the practice. In this paper we seek to address this deficiency by reviewing and quantifying the prominent contributions to the Total Measurement Uncertainty (TMU) budget.

Our work is based mainly on direct experimental work performed using a Canberra model WM2900 TGS [2] but is supported by analytical work and calculations. We discuss sources of both random and systematic uncertainties and how to ameliorate and quantify them for a given assay. Topics covered include: counting statistics; transmission corrections; alignment errors; radial bias; linearity, including the so called 'low mass' bias; partial volume effects, and calibration issues.

INTRODUCTION

The Tomographic Gamma Scanning system or the TGS [1] is a Non-Destructive assay (NDA) technique that combines High Resolution Gamma Spectrometry (HRGS) for net full energy peak determination, with three-dimensional single photon attenuation coefficient images (transmission images) and three-dimensional single photon emission images. This results in improved assay accuracy over non-imaging gamma ray methods certain cases. Three dimensional transmission and emission images are generated by scanning the drum with three degrees of freedom (rotation, translation and elevation) rather than with the two dimensional scanning protocol used in traditional Segmented Gamma Scanners (SGSs). A tomographic image of a waste container is a matrix of 5 state variables; the spatial variables (x, y, z) the gamma-ray energy, E, and the activity (grayness) scale, A. The transmission images are used to correct the emission imaging response matrix for sample specific attenuation losses.

Since the TGS technique corrects for non-uniformities in a matrix distribution as well as in-homogeneities in radionuclide distributions by explicitly measuring the spatial distributions, the

technique is potentially more accurate than traditional non-imaging methods. However, very little information is available in the literature regarding the accuracy of the TGS technique. The objective of this paper is to identify and quantify the prominent sources of random as well as systematic errors that contribute to the TMU budget.

CANBERRA TGS

Working closely with the NIS-6 group (now N2), Canberra Industries has developed the industrial assay platform which implements the mechanical and nucleonics aspects of the TGS approach to best commercial practices. In addition, Canberra has incorporated the data analysis modules into the integrated NDA200 software package, which handles all other aspects of the data acquisition and management.

The Canberra demonstration TGS system uses a large p-type coaxial HPGe detector with a relative efficiency of 120%. This detector is best suited for measuring low activity drums. For higher activity drums, a smaller detector may be beneficial. A fixed-aperture truncated diamond-shaped collimator design was chosen for this study. The collimator height was 60.96 mm and the depth was 152.4 mm. The corners in the horizontal plane had triangular pieces to define a distance of 60.96 mm across the flats. The data acquisition hardware consists of a 16k channel MCA memory card, a Canberra Model 2060 DSP Digital Signal Processing spectroscopy unit, a model 3106D LV/HVPS, and a model 1654 Pulser. The system is supplied with a complete signal processing chain based on Canberra's standard NIM format range.

A ^{152}Eu transmission source of about 7mCi was used to provide a broad energy range of coverage extending from 122 keV to 1408 keV. This encompasses the principal lines commonly used to assay fissile material in drummed waste eg ^{235}U by its 186keV emission and ^{239}Pu by its 129-, 204-, 333-, 375-and 414 keV. In addition it covers the well known ^{137}Cs line at 662 keV and the 1173- and 1332 keV line of ^{60}Co.

The assay protocol is as follows. At the beginning of the assay, the rotator and drum assembly move to a position clear off the line of sight of the detector to the transmission source. The detector lifts are at layer 1 (where the convention is for the bottom layer to be labeled as 0 and the top layer to be labeled as (n-1), n being the number of layers in the scan). An unimpeded spectrum of the transmission source is taken. This measurement not only acts as an energy and efficiency calibration check, but also helps to determine the transmission beam intensity directly (that is without the need to apply a calculated decay correction). Next, measurements are performed at typically n=16 fixed vertical positions corresponding to the mid-height of the 16 layers used in the image analysis. For a 55 U.S. gallon drum, this translates into a layer height of approximately 50 mm. The drum is rotated and translated sideways continuously during the scan of each layer. Data acquisition for each layer begins with the Transmission source/Detector combination close to the edge of the drum. The rotator then begins to move sideways at a constant speed to the center of the drum. Once at the center it reverses direction and moves back to the starting position. The vertical lifts are then raised to the next layer and the sequence is repeated until all layers are complete.

Viewed from above the compass points of the system are as follows: Detector is South; Transmission Source is North, Load/Unload position is West and the vertical lift side of the instrument is on the East. Technically this corresponds to a West scan, with a W-E/E-W translation pattern and a fixed clock-wise rotation, again viewed from above. Figure 1 illustrates the scan pattern used in the assays.

Typically for a nominal 1h assay period, about 112 seconds are spent acquiring data at each of the 16 layers in each of the two modes (Transmission and Emission). Each layer is broken into a 10x10 lattice of square voxels. By convention, based on signal-to-noise and robustness of the analysis arguments, the number of data grabs is set at 1.5 times the number of voxels (i.e. roughly $\pi/2$ times the number of voxels that fit around the drum perimeter). Therefore for each of the 16 vertical layers, 150 measurements are made in order to mathematically over determine the solution for the 10 x 10 voxels in each layer (assuming all data grabs are valid).

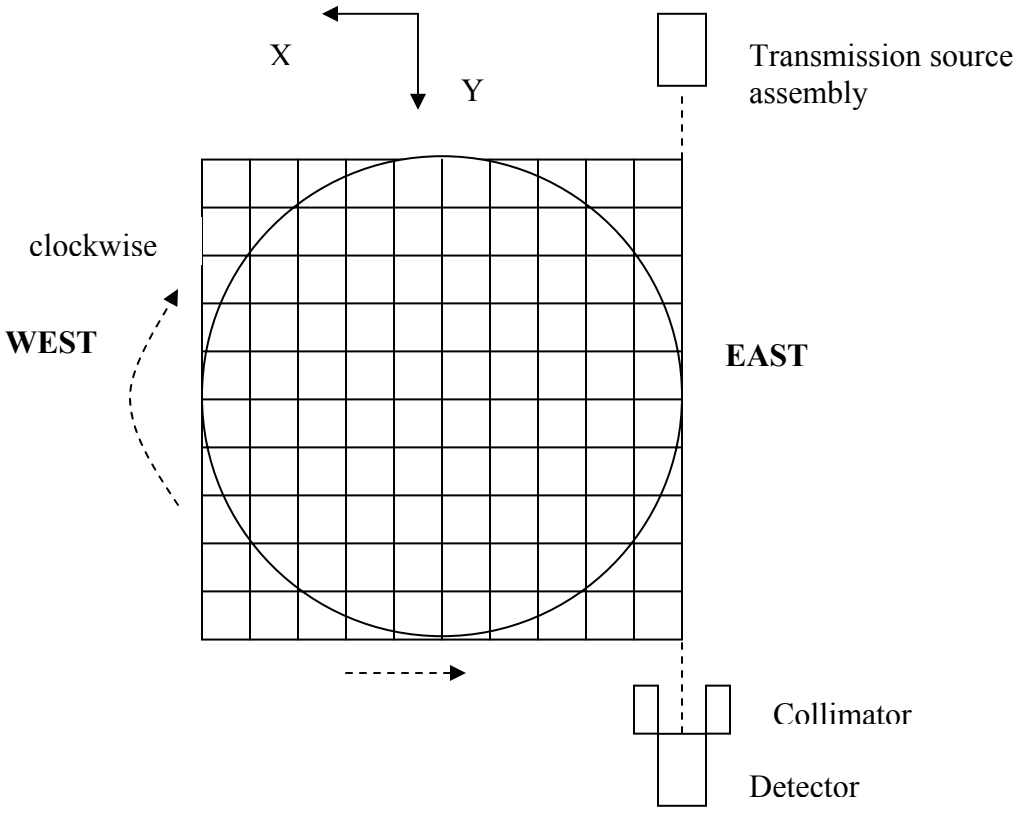

Fig. 1 Canberra TGS scan pattern

MEASUREMENT AND DATA ANALYSES

Prior to the assays, the TGS alignment was checked and fine adjustments were made to the transmission source-HPGe detector alignment. Drums of different matrix types were assayed using a Canberra Model WM2900 TGS. The following drums were assayed; (i) empty, (ii) combustibles (0.17 g.cm^{-3}), (iii) polyethylene (0.61 g.cm^{-3}). Point sources of ^{133}Ba or ^{137}Cs and

^{60}Co were used as emission sources inside the drums. For each drum matrix, TGS measurements were performed as a function of the radial position of the point source.

The TGS Technique

The data were analyzed using the NDA2000 software package that runs the TGS_FIT code developed by the NIS-6 group of LANL. The TGS analysis can be summarized as follows. The linear attenuation coefficient values (μ) for a given drum layer are mapped out over a grid of 10 x 10 voxels. Because the assay items were cylindrical, the 3 voxels in each corner were set to zero in each layer, and 88 voxels per layer were included in the image reconstruction. This represents the transmission image, and is determined by combining the view data obtained during the transmission scan of the given drum layer with the computed path lengths of the transmitted ray through intervening voxels. In the emission part of the analysis, an efficiency matrix is created for each emission voxel at a given photon energy, and is then corrected for attenuation using the transmission image. The view data obtained during the emission scan are combined with the attenuation corrected efficiency matrix to compute the emission image. In other words, the emission image is determined from the following matrix equation.

$$d = F \cdot s \qquad \text{(Eq. 1)}$$

In equation (1), d is an n_{views} vector of measurements, s is an n_{voxels} vector describing the emission image and F is the attenuation corrected efficiency matrix of order n_{views} x n_{voxels}. Unlike the transmission images, in which adjacent drum layers can be considered to be independent, adjacent layers in the emission problem are highly coupled. Because of this strong layer coupling, emission imaging is done 3-dimensionally on the entire sample all at once rather than one layer at a time. The TGS analysis makes use of well-known methods such as Non-Negative Least Squares (NNLS) fit, Algebraic Reconstruction Technique (ART) and Expectation Maximization (EM) to perform image reconstruction. In this work, the ART algorithm was used to fit the transmission image and the EM algorithm was used to fit the emission image.

Another salient feature of the TGS analysis is the use of the so called Material Basis Set (MBS) formalism. The MBS representation allows the energy dependent transmission data (T-data) to be converted to energy independent partial density vectors (ρ data or ρ image). The ρ image vectors can be used to compute transmission images at any energy, in particular at the emission energies. This provides a convenient method for mapping attenuation images from transmission to emission energies [3,4].

An output of a given TGS analysis is a quantity known as the "TGS Number" and the uncertainty associated with it. The TGS number and its uncertainty are determined at each emission energy, and they represent values proportional to the activity or mass of an assayed radionuclide inside the drum.

To illustrate the imaging capability of the Canberra TGS system, the images of a special matrix with the shape of a "wedding cake" are shown in Figure 2. The matrix was created by stacking blocks of wood, with a hole drilled through the middle. Rod sources containing mixed radionuclides were inserted through the central hole in the wedding cake geometry. In Figure 2,

the transmission (linear attenuation coefficient) images are on the left and the emission images are on the right. More specifically, the Transmission images show the linear attenuation coefficient map for the given energy which tracks closely with the matrix density. The bottom images are summed views (similar to radiographs), and the top images are layer slice views. The one layer shown is indicated on the side view by tic marks on either side. The images correspond to the gamma energy of 662 keV.

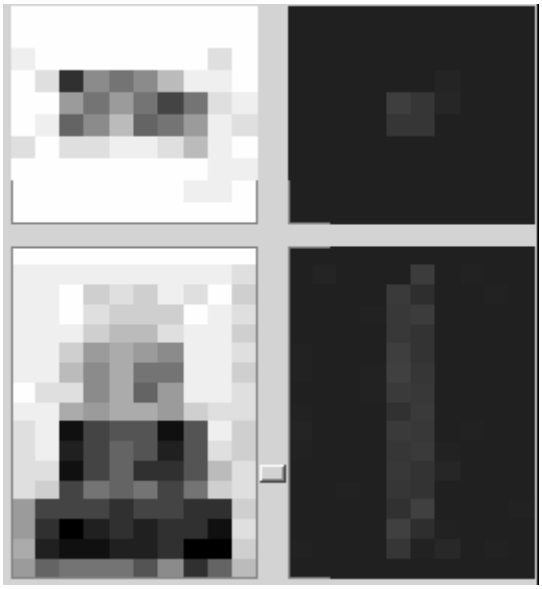

Fig. 2 TGS image of a 'Wedding Cake' geometry

Effective detector position in TGS analysis

The ray-tracing model in TGS assumes the attenuation corrected inverse square law between point sources in the container and the detector. If the Ge crystal is comparable to or smaller than the collimator aperture, the effects of streaming of the higher energy rays through the edges of the crystal become important and give rise to an energy dependence to the effective solid angle. To partially account for this effect (over a narrow energy regime) the TGS ray-tracing model treats the detector as a "black" disk of user specified radius and a user specified distance behind the back face of the collimator. The radius of the disc is set equal to the radius of the active Ge (that is the physical radius less the thickness of the dead-layer). The position of the disc is set behind the end cap inside the Ge crystal itself. For a crystal of active length L, cm, the centroid of interaction is at a distance d_I into the active volume.

$$d_I = \frac{1}{\mu}\left(1 - \frac{\mu L \cdot e^{-\mu L}}{1 - e^{-\mu L}}\right) \qquad \text{(Eq. 2)}$$

The active length of the Ge crystal used in this work was 83.2 mm. For the ^{133}Ba energies, the effective depth of interaction was determined at an average energy of 330 keV and was equal to 16.9 mm. The distance d was estimated to be 24.5 mm. For the ^{137}Cs and ^{60}Co gamma energies, the values of d_I were determined and then averaged. The average value of d_I was 2.50 cm and the distance d was 3.26 cm. In the TGS analyses, the extra distance d was added to the distance

between the axis of rotation and the detector front face. This effectively decreased the geometric efficiency, thus increasing the TGS numbers.

CALIBRATION USING EMPTY DRUM RESULTS

In a real-life waste assay, involving drums with different radionuclide distributions and activities, the TGS system must be calibrated to yield consistent results. The TGS numbers obtained for a known activity or mass of a given nuclide, say in an empty drum, are used as calibration in determining the activity or mass of the nuclide in a matrix drum.

A series of TGS measurements were performed by locating a point source of ^{133}Ba (25 μCi) at different radial positions inside an empty drum. The series of radial measurements were repeated using point sources of ^{137}Cs and ^{60}Co placed in close proximity. The results for the ^{133}Ba gamma lines are given in Table I, along with the statistical uncertainties. The results for the ^{137}Cs and ^{60}Co gamma lines are given in Table II.

Table I TGS Results for a ^{133}Ba point source inside an empty drum

Radial	276 keV		303 keV		356 keV		384 keV	
Position (cm)	TGS no.	Uncertainty	TGS no.	Uncertainty	TGS no.	Uncertainty	TGS no.	Uncertainty
0	0.2398	0.0059	0.5537	0.0091	1.6970	0.0215	0.2363	0.0043
12	0.2475	0.0047	0.5689	0.0082	1.7496	0.0160	0.2384	0.0042
20.5	0.2473	0.0064	0.5870	0.0086	1.8137	0.0340	0.2527	0.0070
26.5	0.2583	0.0065	0.6386	0.0142	1.9129	0.0297	0.2616	0.0093

Table II TGS Results for a ^{137}Cs + ^{60}Co point sources inside an empty drum

Radial	662 keV		1173 keV		1332 keV	
Position (cm)	TGS no.	Uncertainty	TGS no.	Uncertainty	TGS no.	Uncertainty
0	4.6866	0.0441	5.1089	0.0350	4.8927	0.0456
12	4.7091	0.0443	5.0578	0.0475	4.7990	0.0404
20.5	4.9751	0.0482	5.5062	0.0529	5.2439	0.0614
26.5	4.8432	0.0543	5.3158	0.0538	5.0824	0.0362

The statistical uncertainties in the TGS numbers were calculated using the Monte Carlo Randomization (MCR) method [5]. In this method, the counts in the transmission and emission peak regions of interest are randomized, and then the analysis is performed. Several such replicate analyses are conducted using randomized data and the standard deviation in the TGS numbers are calculated. The standard deviation is deemed to be the statistical uncertainty in the measured TGS numbers. Estimating the uncertainties this way is akin to performing repeat measurements and then determining the standard deviation. The MCR method is adopted since no general closed form error propagation formulae are known for EM, ART, and NNLS reconstruction algorithms. In the present work, 20 replicate analyses were done for a given measurement and the uncertainties estimated.

The TGS numbers at the ^{133}Ba gamma ray energies exhibit a radial bias, with the values increasing from the centre to the edge of the drum. The radial bias at the ^{133}Ba gamma ray

energies was in the range from 7% to 15%. The TGS results at ^{137}Cs and ^{60}Co gamma energies also exhibited a radial bias, although the trend was different. The TGS numbers increased initially as one moved from the centre towards the edge of the drum, reached a maximum at a radius value equal to 70% of the drum radius, and then decreased. The magnitude of the bias at 662 keV was 6% approximately, and the bias at 1173 keV and 1332 keV were in the 7%-8% range.

A radial weighting scheme was adopted to calculate an average TGS number at each gamma ray energy for the empty drum case. The radial weighted average was calculated as follows.

$$TGS_{Avg}(E) = \frac{\sum_i W_i \cdot TGS_i}{\sum_i W_i} \tag{3}$$

In equation (4), TGS_i is the TGS number measured at the i-th radial position and W_i is the weighting factor at the i-th radius.

The uncertainty in the weighted average was calculated based on the *average variance* of the results. The expression for average variance is given in equation (4).

$$\sigma^2 = \left(\frac{N}{N-1}\right)\frac{\sum_i Wi\left(TGS_i - TGS_{Avg}\right)^2}{\sum_i W_i} \tag{4}$$

In equation (4), N is the number of radial measurements. The uncertainty in the weighted average is therefore,

$$\sigma_{wtdAvg} = \frac{\sigma}{\sqrt{N}} \tag{5}$$

The calibration parameters were obtained by dividing the average TGS number by the nuclide activity in the standard source. The average TGS numbers and the calibration parameters for the ^{133}Ba gamma ray energies are given in Table III, and those for ^{137}Cs and ^{60}Co energies are given in Table IV.

Table III Calibration parameters for ^{133}Ba gamma energies

Energy (keV)	276	303	356	384
$TGS_{Avg}(E)$	0.2516	0.6038	1.8397	0.2533
Uncertainty	0.0032	0.0170	0.0376	0.0050
$TGS_{Avg}(E)/\mu Ci$	0.01007	0.02415	0.07359	0.01013
Rel. Uncertainty	1.26%	2.81%	2.04%	1.97%

Table IV Calibration parameters for ^{137}Cs and ^{60}Co gamma energies

Energy (keV)	662	1173	1332
$TGS_{Avg}(E)$	4.8673	5.3385	5.0890
Uncertainty	0.0578	0.0950	0.0933
$TGS_{Avg}(E)/\mu Ci$	0.04867	0.07118	0.06785
Rel. Uncertainty	1.19%	1.78%	1.83%

Alleviating Radial bias using an offset parameter in the analysis

It was observed that the radial bias in the TGS numbers from the empty drum became smaller if an offset parameter in the –X direction was included in the analysis. For example, when an offset parameter of –9.525 mm (or 3/8 inches) was used, the bias in the TGS numbers decreased considerably. The magnitude of the bias at 276, 303, 356, and 384 keV were, respectively, 2.2%, 7.2%, 4.5%, and 5.1%. The bias in the TGS numbers at 662 keV was 3.2%, and at 1173 and 1332 keV it was 5.1% and 3.6%, respectively. The radial bias in the TGS numbers at every energy decreased when an offset parameter was used.

An offset would only be necessary if the transmission source and the detector were misaligned in the X direction relative to the extent of the mechanical scan and/or the TGS collimator assembly was not perpendicular to the axis of rotation. The Canberra TGS system was aligned with great care, with the alignment being checked periodically. The tolerances were very small, typically within 1 mm. Because of these reasons, it was not conceivable that the system was misaligned by as much as 10 mm. No X-offset parameter was therefore included in the analysis. Any improvement in using a finite offset must arise because of the effect it has on ameliorating modeling approximations.

TGS RESULTS FOR LIGHT AND MODERATELY DENSE MATRIX DRUMS

The calibration parameters (Tables III and IV) derived using the empty drum measurements were applied to the TGS results from the matrix drums. The activity results for a ^{133}Ba point source in a combustibles matrix drum (0.17 gcm^{-3}) are given in Table V. The results for ^{137}Cs and ^{60}Co are given in Table VI. The results for a polyethylene matrix drum (0.61 gcm^{-3}) are given in Tables VII and VIII. The uncertainties in the nuclide activities are the quadrature sum of the random uncertainties calculated using the MCR method, and the uncertainties in the calibration parameter.

Table V TGS Results for a 25 μCi ^{133}Ba point source inside a combustibles matrix drum

Radial Position (mm)	276 keV		303 keV		356 keV		384 keV	
	Activity (μCi)	Uncertainty (μCi)	Activity (μCi)	Uncertainty (μCi)	Activity (μCi)	Uncertainty (μCi)	Activity (μCi)	Uncertainty (μCi)
0	23.30	0.64	22.47	0.84	22.88	0.68	22.38	0.82
120	22.99	0.71	23.25	0.79	23.58	0.67	24.12	0.94
205	24.16	0.76	24.29	0.89	25.85	0.87	25.49	0.95
265	23.70	0.88	24.83	0.84	25.58	0.64	25.06	0.64

Table VI TGS Results for a ^{137}Cs (100 μCi) + ^{60}Co (75 μCi) point sources inside a combustibles drum

Radial Position (mm)	662 keV		1173 keV		1332 keV	
	Activity (μCi)	Uncertainty (μCi)	Activity (μCi)	Uncertainty (μCi)	Activity (μCi)	Uncertainty (μCi)
0	96.07	2.31	71.20	1.65	70.59	1.63
120	98.36	1.69	73.63	1.43	73.49	1.46
205	100.65	2.04	75.71	1.68	75.28	1.67
265	109.92	2.09	77.69	1.64	78.54	1.70

For the combustibles drum, the activity results at a given gamma energy are biased low at radial positions closer to drum center, and are biased high at positions near the edge of the drum. The bias magnitudes are similar to those observed in the case of the empty drum. The transmission and emission images for the ^{133}Ba point source located at a radius of 205 mm are shown in Figure 3. The images correspond to a gamma ray energy of 356 keV. The emission image is sharp and appears to be contained within two voxels.

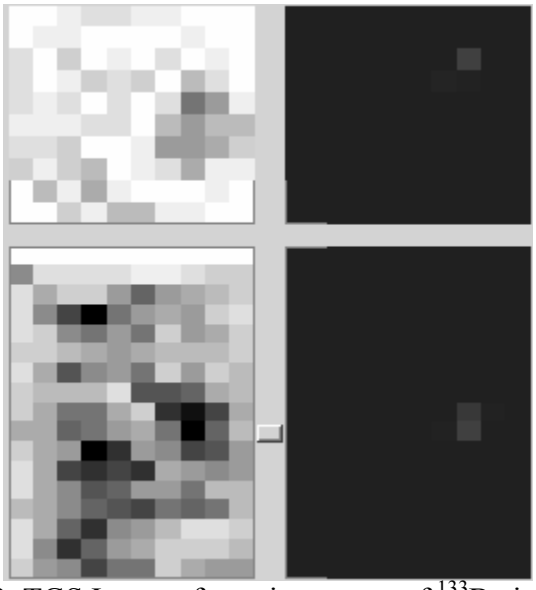

Fig. 2 TGS Images for point source of ^{133}Ba inside a Combustibles drum

Table VII TGS Results for a 25 μCi ^{133}Ba point source inside a Polyethylene matrix drum

Radial Position (mm)	276 keV		303 keV		356 keV		384 keV	
	Activity (μCi)	Uncertainty (μCi)	Activity (μCi)	Uncertainty (μCi)	Activity (μCi)	Uncertainty (μCi)	Activity (μCi)	Uncertainty (μCi)
0	13.29	1.64	17.79	1.22	20.20	1.44	16.87	1.00
120	18.66	1.61	18.00	1.13	20.28	1.36	20.05	0.95
205	21.27	1.58	21.41	1.22	21.44	1.29	20.76	1.12
265	29.57	1.80	29.90	1.73	28.22	1.59	28.24	1.66

Table VIII TGS Results for a ^{137}Cs (100 μCi) + ^{60}Co (75 μCi) point sources inside a Polyethylene drum

Radial Position (mm)	662 keV		1173 keV		1332 keV	
	Activity (μCi)	Uncertainty (μCi)	Activity (μCi)	Uncertainty (μCi)	Activity (μCi)	Uncertainty (μCi)
0	84.04	4.12	63.38	2.69	63.59	2.58
120	93.09	4.02	68.68	2.45	69.29	2.63
205	87.39	4.75	68.99	3.21	69.32	2.99
265	109.83	5.06	78.00	2.57	76.56	2.48

For the polyethylene matrix, the TGS results at lower energies (276 keV – 384 keV) are once again biased low at locations close to the center and are biased high at positions closer to the edge of the drum. The magnitudes of the biases are significantly higher than those observed in the case of the empty or combustibles drum.

In the case of matrix drums, the radial bias is suspected to be primarily due to the spreading of the emission image to neighbouring voxels, with the consequence of an erroneous transmission being applied. Poor counting statistics in the view data from the emission scan is the dominant reason for the spreading of an emission image. The error induced would be more serious for dense matrices and at lower gamma ray energies, owing to greater photon attenuation. For example, for a single point source of energy 303 keV, the photon transmission through polyethylene over a length of a voxel (6 cm) is 0.6. Therefore, the spreading of the emission image over a voxel would introduce an error of 66%.

At ^{137}Cs and ^{60}Co gamma ray energies, the TGS results for the polyethylene matrix exhibit much smaller biases than those observed at the ^{133}Ba gamma energies. The reasons could be because of better counting statistics in the emission data resulting in a smaller spread of the image. For example, at the gamma energy of 662 keV, the photon transmission over the length of a voxel is 0.69. For the 1332 keV gamma ray, the photon transmission is 0.77. Therefore, for a single point source, the magnitudes of the errors at 662 keV and 1332 keV are 44% and 29%, respectively.

The error induced due to poor counting statistics in emission data is compounded by uncertainties in the transmission image. Uniform matrices, such as the polyethylene matrix used in this work, lack image contrast and are inherently difficult to reconstruct. The net effect is that the map of linear attenuation coefficients μ, wanders about the mean value somewhat randomly to create a 'checker board' pattern. This makes the matrix less attenuating and results in a low bias that gets worse as the density increases, and is also worse toward the center.

The images shown in Figure 3 illustrate the spreading of the emission image, as well as the checker board pattern observed in the transmission image. The images correspond to a point source of ^{133}Ba (356 keV) at a radius of 12 cm within a polyethylene matrix drum. The emission image is spread over several voxels.

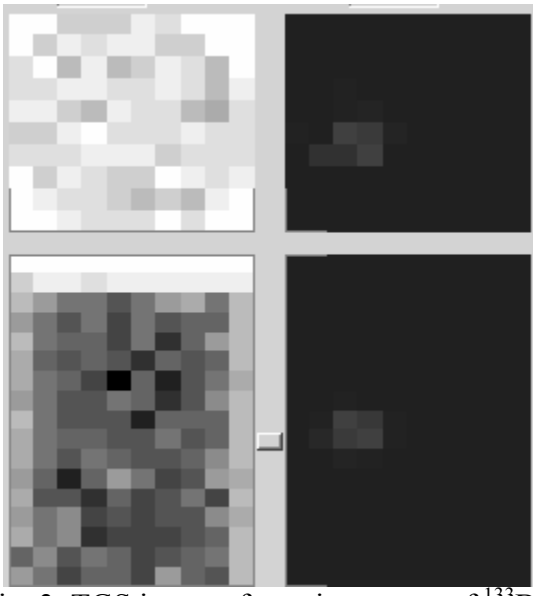

Fig. 3 TGS images for point source of ^{133}Ba inside a Polyethylene drum

THE TOTAL MEASUREMENT UNCERTAINTY (TMU) BUDGET

For TGS assays of drums with light to moderately dense matrices, the major contributions to the Total Measurement Uncertainty (TMU) budget are quantified in this section.

Statistical Errors

The statistical uncertainties in the TGS results were estimated using the Monte Carlo Randomization method. For the combustibles matrix, the statistical uncertainties were 2%-3% at all energies that were considered. For the polyethylene matrix, the statistical uncertainties were 7%-8% at the ^{133}Ba energies, and were 5% at ^{137}Cs and ^{60}Co energies.

Poor counting statistics in the transmission and emission view data will result in a significant systematic bias in the TGS results with the errors being much larger than the random uncertainty estimated using the MCR method.

Calibration Uncertainties

The uncertainties in the calibration parameters are given in Tables 3 and 4. The calibration uncertainties are in the 1%-3% range.

The uncertainties quoted in the TGS results given in Tables V through VIII are the statistical and calibration uncertainties summed in quadrature.

Source location errors

The error due to source location was derived using the point source nuclide activities measured at various radial locations. First, the deviation of the measured point source activity with respect to the true activity was determined and squared. Next, the squared deviation was weighted using a factor that was dependent on the probability of the source being located in a voxel that was within an annulus between two radii.

The average variance in the activity, attributable to source location is determined from the following equation.

$$\sigma^2_{\text{source-location}} = \frac{\sum_i w_i (A_i - A_{\text{True}})^2}{\sum_i w_i} \qquad \text{(Eq. 6)}$$

In equation (6), the index 'i' refers to the radial location. The deviation is taken with respect to the true activity of the source, rather than an *estimate* of the true activity. The average variance calculated from equation (6) is for a single point source. Based on the postulate that a typical waste drum is likely to contain at least 3 equivalent point sources randomly distributed in the drum volume, the error due to source location is calculated as follows.

$$\sigma_{\text{source-location}} = \frac{1}{\sqrt{3}} \sqrt{\frac{\sum_i w_i (A_i - A_{\text{True}})^2}{\sum_i w_i}} \qquad \text{(Eq. 7)}$$

The relative uncertainties due to source location are given in Table IX.

Table IX Relative uncertainty due to source location

Energy (keV)	Relative uncertainty due to source location	
	Combustibles (0.17 g.cm^{-3})	Polyethylene (0.61 g.cm^{-3})
300-400	1.3%	5.9%
662	2.1%	3.6%
1173	0.9%	2.3%
1332	1.1%	2.1%

Matrix Errors

To estimate the matrix error due to the checkerboard effect, the TGS results based on a reconstructed transmission image was compared against a simulated transmission image. For the combustibles and polyethylene matrices, the matrix error in the energy range of interest was estimated to be 5% and 7%, respectively.

Method Error

The response model used in the TGS analysis assumes that the activity distribution can be described by locating point sources at the center of each voxel. If a source happens to be present at the boundary of two voxels, the TGS analysis will distribute the activity within the two voxels. The classic case is a point source located at the center of the drum. Since there is no central voxel in a 10 x 10 array, the source placement that results from the assay is necessarily distributed into (at best) the middle four voxels. Thus the source activity is, on the average, displaced outward. This results in an attenuation correction factor that is smaller than the true value and a systematic under-estimation of the activity present.

For source locations at voxel boundaries near the edge of the drum, the activity will be displaced towards an inward voxel, thus resulting in a larger attenuation correction factor. The activity present is over-estimated.

This effect is independent of counting statistics and will be present even when the emission and transmission data have very good counting precision. This is an inherent limitation of the method.

The error contribution is estimated as follows. Defining the average linear attenuation coefficient taken over all voxels in a drum layer as μ, and the voxel width by x, the attenuation factor across a 'typical' voxel is given by the following equation.

$$f\_vox = e^{-\mu x} \qquad \text{(Eq. 8)}$$

In terms of the diametrical transmission factor, T, commonly used in SGS matrix correction parlance we can write,

$$f\_vox = T^{x/d} \qquad \text{(Eq. 9)}$$

Where d is the drum diameter.

The error induced due to the displacement of the emission image by a voxel width will be (1/f_vox-1). Further, it is postulated that a typical waste drum is likely to contain at least three equivalent point sources randomly distributed in the drum volume. The 1-σ relative standard deviation can be approximated as,

$$\Delta_{method} = \frac{\left(1/f\_vox - 1\right)}{6 \cdot \sqrt{3}} \qquad \text{(Eq. 10)}$$

Equation (9) represents the $\pm 1\sigma$ band of uncertainty that covers the under-estimation and the over-estimation of activity for 3 equal point sources randomly distributed in the drum volume. The results are given in Table X.

Table X Method Errors

Energy (keV)	Method Errors – Relative Standard Deviation	
	Combustibles (0.17 g.cm^{-3})	Polyethylene (0.61 g.cm^{-3})
300-400	1.2%	4.6%
662	0.9%	3.3%
1173	0.7%	2.4%
1332	0.6%	2.2%

Other Error Contributions to TMU

Besides the errors already discussed, there could be other contributions to the TMU in a TGS assay. These are from errors due to misalignment, partial volume effects, self-attenuation in lumps of source activity (typically much smaller than a voxel size), and the "low mass" bias effect. Each of these is discussed in turn.

Misalignment

Misalignment in TGS can be defined as the difference between the actual geometry of the scanner and the assumed geometry used to compute the transmission and emission response matrices for image reconstructions. Misalignments can lead to a significant assay bias. The fundamental types of misalignments in TGS emission scanning are given below.

(i) A transverse offset between the detector/collimator center line and the sample center of rotation in the presumed x=0 position
(ii) An incorrect specification of the virtual detector offset that gives the distance between the detector end cap and crystal plus the mean penetration depth of the photons
(iii) A pitch of the transverse motion direction relative to the x-axis (which is defined to be normal to the collimator axis) in the horizontal XY plane.
(iv) The axis of the sample offset with respect to the center of rotation (for e.g. a wobbly drum).

In the present case, the scanner was not misaligned in any way. Therefore, no errors due to misalignment were included in the TMU budget. In a general case, the scanner could be misaligned in one or more ways as described above. The magnitude of bias caused by misalignments of type (i)-(iii) can be estimated by the computational methods given in reference [6].

In the present work, alignment errors of type (iv) were estimated by deliberately mis-positioning the drum on the rotator. An offset of ±15 mm of the drum axis with respect to the center of rotation yielded an average bias of ±3.0% (or ±0.2% per mm).

Partial Volume Effect

In a waste matrix where there is a significant non-uniformity within a given vertical layer, it is possible that the highly collimated transmission beam only traverses a partial volume of the layer. This will result in a bias in the attenuation values that are calculated for the voxels in the given layer. For example, if the drum is not filled with a matrix material up to the brim, the topmost layer will only be partially full. The transmission beam may only traverse the filled

portion of the layer, thus resulting in higher attenuation values for the voxels in the top layer. The activity of a source present in these voxels will, therefore, be over-estimated. In the present work, the matrices were fairly uniform, and sources were located at roughly half the height of the drum, (i.e.) buried inside the matrix. No error due to partial volume effect was therefore included in the TMU.

In the general case, however, an additional contribution must be carried to account for the mismatch between modeling the item as a stack of boxes uniformly filled with matrix with an ideal point source of activity at their center. In fact, the curved surface of the drum guarantees a mismatch for the outer voxels. The redeeming feature is that the scanning protocol averages the material properties over many views or data grabs.

Self-attenuation

Self-attenuation generally only affects the accuracy of the Pu and U measurements when they are present in lumps due to the special combination of high atomic number, high density and weakly penetrating gamma rays. Self-attenuation results in under-reporting relative to a calibration referred to ideal or dilute conditions. Self-attenuation errors are difficult to calculate with confidence, except for the worst-case measurement conditions which is a spherical metallic source. However, this geometry is not likely and therefore a realistic self-attenuation error would tend to be much smaller.

Since the TGS system will be used primarily for the low gram level measurements, the worst-case self-absorption error is only a few percent and most likely would be close to zero if calibrated with somewhat representative sources. At the 1-gram level the worst-case self-absorption error would be approximately 60%. At this level the combination of the multiple gamma line assays would flag the waste drum as a potential assay problem in the standard data review. For U the effects occur at lower U loadings because the 186keV gamma-ray line is from the decay of ^{235}U is so weakly penetrating. There is no practical means within TGS to flag or reliably compensate for the effect in this case.

In the present work, the calibrations were performed using the same sources as those that were assayed inside different matrices. Therefore, the error due to self-attenuation effects would be zero.

Low Mass Bias

The phrase ‘low mass bias’ has been informally used in TGS assays to describe systematic errors that arise from zero truncation in the emission image reconstruction. Emission image reconstruction algorithms used in TGS are constrained to give a non-negative result in every image voxel. Therefore, repeated assays of samples with low masses or activities can give results that are high on average. The effect is strictly dependent on the signal to noise ratio of the item and can therefore also be exacerbated by a high continuum background below the peak of interest. The TGS methodology used here, as developed by one of the authors (Robert Estep), circumvents this problem by requiring that the image reconstruction algorithm preserve the total count rate in reverse projection [7]. This is achieved by a simple normalization of the mass image.

If an image reconstruction algorithm used in some TGS method does not address and correct for the low mass bias problem, then an appropriate error due to this effect should be added to the TMU. In the present work, the algorithms used in the TGS analyses were forced to preserve the total count rates in forward and reverse projections, and therefore, the error due to the effect of 'low mass bias' is zero.

SUMMED UNCERTAINTY ESTIMATE FOR THE TGS SYSTEM

The uncertainty for each of the error sources discussed above is added in quadrature and scaled to derive a 95% confidence limit.

$$\sigma_{TMU} = 1.96 \cdot A \cdot \sqrt{\sigma^2_{calibratio\ n} + \sigma^2_{random} + \sigma^2_{matrix} + \sigma^2_{source-location} + \sigma^2_{method}} \qquad \text{(Eq. 11)}$$

TMU estimates at the 1-σ level are evaluated using the same expression but with the multiplier 1.96 replaced by unity.

The TMU estimates for combustibles and polyethylene matrices at 1-σ level are given in Tables XIa and XIb, respectively.

Table XIa TMU estimates for combustibles matrix

Energy (keV	Source of Uncertainty					TMU (1σ)
	Calibration	Random	Method	Matrix	Source location	
300-400	2.0%	3.0%	1.2%	5.0%	1.3%	6.41%
662	1.2%	2.0%	0.9%	5.0%	2.1%	5.97%
1173	1.8%	2.0%	0.7%	5.0%	0.9%	5.79%
1332	1.8%	2.0%	0.6%	5.0%	1.1%	5.81%

Table XIb TMU estimates for polyethylene matrix

Energy (keV	Source of Uncertainty					TMU (1σ)
	Calibration	Random	Method	Matrix	Source location	
300-400	2.0%	7.5%	4.6%	7.0%	5.9%	12.85%
662	1.2%	5.0%	3.3%	7.0%	3.6%	9.96%
1173	1.8%	5.0%	2.4%	7.0%	2.3%	9.40%
1332	1.8%	5.0%	2.2%	7.0%	2.1%	9.30%

CONCLUSIONS AND FUTURE WORK

The performance of Canberra TGS system was discussed for light and moderately dense waste matrices. The various sources of errors were identified and their magnitudes were quantified. Measurements were performed at several radial locations, using a single point source of a given nuclide. The results indicated a radial bias with the activities biased low towards the center of the drum, and biased high towards the edge of the drum. The bias was worse at lower energies and for a denser drum. The primary reason for the bias is thought to be due to the spreading of the emission image to neighboring voxels. This spreading tends to increase as the counting statistics

in the view data worsens. However, it must be noted that it is unlikely that a typical waste drum will contain a single point source. For a typical waste drum with at least three equal point sources, the maximum error due to source location was a modest 5.9%.

For high-density drums, additional sources of uncertainty begin to play a more dominant role. This will be discussed in future works.

Poor counting statistics can also affect the transmission image via the checkerboard effect and can lead to an under-estimation of nuclide activity. Various smoothing techniques are being explored in order to alleviate the checkerboard effect in the transmission image. Ultimately, however, the transmission image reconstruction for a given scanner and assay time is limited by the viability of the transmission grab data through the item. Initially, low transmission values can be dropped without much impact. Ultimately, the opacity of large parts of the drum becomes prohibitive. The emission image related errors also pose a much more serious problem, especially at high matrix densities (1.0 $g.cm^{-3}$ and higher). Various options are being considered to address this problem and will be reported elsewhere.

Measurements using a variety of source distributions and different matrix types have been made and are in progress at Canberra Industries. Measurements are also being performed using dense matrices such as Sand (density=1.8 $g.cm^{-3}$). Results from these will be presented in the future.

REFERENCES

1 R.J. Estep, *Assay of heterogeneous radioactive wastes by low-resolution tomographic gamma scanning*, ANS Transactions **62**(1990) 178.

2 S. Croft, TD Anderson, R.J. Estep, R.J. Huckins, D.L. Petroka, R. Venkataraman and M. Villani, *A new drum tomographic gamma scanning system*, Presented at the 25th ESARDA Symposium on Safeguards and Nuclear Material Management, Stockholm, Sweden, 13-15 May 2003.

3 R.J. Estep, T.H. Prettyman, and G.A. Sheppard, *Comparison of attenuation correction methods for TGS and SGS: Do we really need Selenium-75?*, Proceedings of 35th INMM Annual Meeting, Naples, FL, July 1996.

4 R.S. Thomason and S.Croft, *Computational study of the accuracy of the Material Basis Set method for transmission data interpolation*, Proceedings of 44th Annual INMM Meeting, Phoenix, AZ, July 2003.

5 R.J. Estep, D.Miko, and S. Milton, *Monte Carlo error estimation applied to Nondestructive Assay methods*, Nondestructive Assay Waste Characterization Conference, Salt Lake City, Utah, May 22-26, 2000.

6 R.J. Estep, L. Foster, D. Miko, J. Rennie, S. Dittrich, and S. Croft, *Diagnostic scanning procedures to identify and correct for misalignment in Tomographic Gamma Scanners (TGS)*, Proceedings of the 43rd Annual INMM Meeting, Orlando, FL, June 2002.

7 R.J. Estep, R. Brandenburg, and J. Wachter, *Low-Mass bias issues in Tomographic Gamma Scanning (TGS)*, Proceedings of the 42nd Annual INMM Meeting, Indian Wells, CA, July 2001.